

# Nitric oxide modulates the influx of extracellular Ca<sup>2+</sup> and actin filament organization during cell wall construction in *Pinus bungeana* pollen tubes

Yuhua Wang<sup>1,2,3</sup>, Tong Chen<sup>1</sup>, Chunyang Zhang<sup>1,2</sup>, Huaiqing Hao<sup>1</sup>, Peng Liu<sup>1,2</sup>, Maozhong Zheng<sup>1,2</sup>, František Baluška<sup>4</sup>, Jozef Šamaj<sup>4,5,6</sup> and Jinxing Lin<sup>1</sup>

<sup>1</sup>Key Laboratory of Photosynthesis and Molecular Environmental Physiology, Institute of Botany, Chinese Academy of Sciences, Beijing 100093, China;

<sup>2</sup>Graduate School of Chinese Academy of Sciences, Beijing 100049, China; <sup>3</sup>The College of Horticulture, Nanjing Agricultural University, Nanjing 210095,

China; <sup>4</sup>Institute of Cellular and Molecular Botany, Rheinische Friedrich-Wilhelms-University Bonn, Department of Plant Cell Biology, Kirschallee 1, D-53115

Bonn, Germany; <sup>5</sup>Institute of Plant Genetics and Biotechnology, Slovak Academy of Sciences, Akademicka 2, SK-95007, Nitra, Slovak Republic; <sup>6</sup>Palacky

University Olomouc, Faculty of Natural Science, Olomouc 771 46, Czech Republic

## Summary

Author for correspondence:

Jinxing Lin

Tel: 0086 10 62836211

Email: linjx@ibcas.ac.cn

Received: 5 November 2008

Accepted: 3 February 2009

*New Phytologist* (2009) **182**: 851–862

doi: 10.1111/j.1469-8137.2009.02820.x

**Key words:** actin filaments, calcium influx, cell wall, nitric oxide (NO), pollen tube.

- Nitric oxide (NO) plays a key role in many physiological processes in plants, including pollen tube growth. Here, effects of NO on extracellular Ca<sup>2+</sup> flux and microfilaments during cell wall construction in *Pinus bungeana* pollen tubes were investigated.
- Extracellular Ca<sup>2+</sup> influx, the intracellular Ca<sup>2+</sup> gradient, patterns of actin organization, vesicle trafficking and cell wall deposition upon treatment with the NO donor S-nitroso-N-acetylpenicillamine (SNAP), the NO synthase (NOS) inhibitor N<sub>ω</sub>-nitro-L-arginine (L-NNA) or the NO scavenger 2-(4-carboxyphenyl)-4, 4, 5, 5-tetramethylimidazole-1-oxyl-3-oxide (cPTIO) were analyzed.
- SNAP enhanced pollen tube growth in a dose-dependent manner, while L-NNA and cPTIO inhibited NO production and arrested pollen tube growth. Noninvasive detection and microinjection of a Ca<sup>2+</sup> indicator revealed that SNAP promoted extracellular Ca<sup>2+</sup> influx and increased the steepness of the tip-focused Ca<sup>2+</sup> gradient, while cPTIO and L-NNA had the opposite effect. Fluorescence labeling indicated that SNAP, cPTIO and L-NNA altered actin organization, which subsequently affected vesicle trafficking. Finally, the configuration and/or distribution of cell wall components such as pectins and callose were significantly altered in response to L-NNA. Fourier transform infrared (FTIR) microspectroscopy confirmed the changes in the chemical composition of walls.
- Our results indicate that NO affects the configuration and distribution of cell wall components in pollen tubes by altering extracellular Ca<sup>2+</sup> influx and F-actin organization.

## Introduction

Pollen tubes are tip-growing cells that grow relatively quickly within the female gametophyte to deliver sperm nuclei for fertilization. Thus, pollen tubes are an essential part of sexual reproduction in higher plants (Hepler *et al.*, 2001). Recent studies have indicated that the tip-focused cytoplasmic Ca<sup>2+</sup> gradient, the regulation of actin cytoskeleton organization and polar vesicular trafficking are critical components of the tip-growth mechanism in pollen tubes (Hepler *et al.*, 2001; Šamaj *et al.*, 2004). Disruption of the tip-focused Ca<sup>2+</sup> gradient in pollen tubes leads to cessation of tip growth and formation of

extensive actin filament bundles in the tip region (Lancelle *et al.*, 1997), suggesting that higher concentrations of Ca<sup>2+</sup> at the tips of pollen tubes suppress actin filament bundle formation (Yokota *et al.*, 2000). In addition, the construction and composition of the cell wall and the configuration of its building materials are important features that regulate pollen tube growth (Chen *et al.*, 2007). Furthermore, secretory vesicles move to areas of higher Ca<sup>2+</sup>, where the vesicles accumulate and release cell wall precursors by fusion to the membrane, subsequently resulting in cell wall expansion and cell growth (Holdaway-Clarke *et al.*, 1997; Camacho & Malhó, 2003).

In recent years, nitric oxide (NO) has been described as a highly active gaseous signaling molecule with multiple biological functions in plants (Courtois *et al.*, 2008), including stimulation of seed germination (Beligni & Lamattina, 2000), root formation (Lanteri *et al.*, 2008) and other processes of plant growth and development (Guo & Crawford, 2005), and regulation of stomatal movement (Neill *et al.*, 2008). NO is also involved in highly polarized tip growth. For example, endogenous NO plays a positive role in root hair formation in *Arabidopsis* and *Lactuca sativa* by taking part in the auxin response (Lombardo *et al.*, 2006). Recently, Salmi *et al.* (2007) reported that NO plays a signaling role in gravity-directed cell polarity in germinating *Ceratopteris richardii* spores. With respect to pollen tube growth, NO is involved in the growth regulation and reorientation of *Lilium longiflorum* and *Arabidopsis* pollen tubes (Prado *et al.*, 2004, 2008). In addition, NO is thought to be involved in pollen–stigma interactions and defense in angiosperms (McInnis *et al.*, 2006), and to play an inhibitory role in pollen germination and tube growth in *Paulownia tomentosa* in response to UV-B light (He *et al.*, 2007). Previous reports have indicated that intracellular signaling via NO involves generation of cyclic guanosine monophosphate (cGMP) and cyclic ADP ribose (cADPR) and elevation of cytosolic  $\text{Ca}^{2+}$  (Lanteri *et al.*, 2006). However, in many cases, NO-dependent physiological responses are governed by a complex signaling network, for which the biochemical and molecular mechanisms have not been deciphered (Neill *et al.*, 2008). Furthermore, there are no data currently available to support the involvement of NO in cell wall construction of pollen tubes. Therefore, we investigated the regulatory roles of NO during pollen tube development in the gymnosperm *Pinus bungeana*. Specifically, we focused on the concentrations of NO in pollen tubes, as well as several linked cellular features that are essential for pollen tube tip growth, including extracellular  $\text{Ca}^{2+}$  uptake and the cytoplasmic  $\text{Ca}^{2+}$  gradient, actin filament (AF) organization, and the composition of the cell wall during NO induction, or in response to pharmacological disturbance of NO production.

## Materials and Methods

### Plant material

Mature pollen was collected from *Pinus bungeana* Zucc. trees growing in the Botanical Garden of the Institute of Botany, Chinese Academy of Sciences, in May 2007 and stored at  $-20^{\circ}\text{C}$ . *In vitro* pollen culture was performed by liquid mass culture. After 30 min of rehydration at room temperature under 100% relative humidity, pollen grains were suspended in germination medium containing 15% sucrose, 0.01%  $\text{H}_3\text{BO}_3$ , and 0.01%  $\text{CaCl}_2$  at pH 6.8 on a shaker (121 rpm) at  $25^{\circ}\text{C}$  in the dark. The NO synthase (NOS) inhibitor  $N_{\omega}$ -nitro-L-arginine (L-NNA) was dissolved in 0.5 N HCl, while the NO donor S-nitroso-N-acetylpenicillamine (SNAP) and the scavenger 2-(4-carboxyphenyl)-4, 4, 5, 5-tetramethylimidazole-1-oxyl-3-

oxide (cPTIO) were dissolved in double-distilled water ( $\text{ddH}_2\text{O}$ ) and then added to the culture medium after pollen grains had been cultured for 60 h in standard medium. The pollen tubes were subjected to further incubation for another 24 h in the presence of different concentrations of drugs. For the germination experiment, various concentrations of SNAP, cPTIO and L-NNA were added to the medium from the beginning of culture and the germination percentage was calculated after 60 h. Moreover, the control was cultured in the presence of HCl, and all working concentrations of HCl were below  $10^{-4}$  mol, a level necessary to dissolve L-NNA; there were no obvious effects on pollen germination or tube growth.

### Pollen tube growth determination and morphological observation

To measure the mean tube length, at least 50 pollen tubes were detected in each of five replicates at 12-h intervals. Pollen grains were not considered germinated unless the tube length was greater than the diameter of the grain. The morphology of pollen tubes was examined with a Zeiss Q500 IW light microscope, and digital images were captured with a Spot II camera (Zeiss, Göttingen, Germany).

### NO assays and NO imaging

The presence of NO in pollen tubes was assayed and visualized as previously described with small modifications (Prado *et al.*, 2004). Samples were incubated in  $5\ \mu\text{M}$  4, 5-diaminofluorescein diacetate (DAF-2DA; Merck, San Diego, California, USA) for 15 min and then excess fluorophore was washed out. The specimens were examined using a 488-nm argon laser under a confocal laser-scanning microscope (CLSM Zeiss 510 META) with the same parameter settings. Emission signals were collected at 500–550 nm. The relative fluorescence intensities of at least 50 pollen tubes in each of five replicates were measured using IMAGEJ (NIH, Bethesda, Maryland, USA), and mean relative fluorescence intensities were calculated.

### Measurement of cytoplasmic $\text{Ca}^{2+}$

Pollen tubes were pressure-injected with 2.5 mM Calcium Green-1 dextran (MW = 10 000; Molecular Probes Inc., Eugene, OR, USA) in 5 mM Hepes buffer (pH 7.0). The pipette tip reached no more than  $3\ \mu\text{m}$  into the cytoplasm of the pollen tubes, and the agents were gently loaded into the cytoplasm within *c.* 5 min, then the micropipette was slowly removed from the cell within *c.* 30 min to allow the cell to form a plug that healed the wound, and resume normal growth, thus guaranteeing that no cytoplasm was lost. Pollen tubes that suffered severe mechanical damage or leakage of cytoplasm were discarded. The samples were then excited with a 488-nm argon laser using the CLSM and emission signals were collected at 500–550 nm. Image analysis was carried out with CLSM 510

META software. The 'steepness' of the tip-focused  $\text{Ca}^{2+}$  gradient was employed to describe the effects of NO-modulating drugs on the maintenance of the tip-focused  $\text{Ca}^{2+}$  gradient (Lazzaro *et al.*, 2003) (Supporting Information, Fig. S1). To determine whether injection affected pollen tube growth, Hepes buffer was microinjected into normally growing pollen tubes as a control injection.

#### Measurement of pollen tube tip extracellular $\text{Ca}^{2+}$ fluxes

Net  $\text{Ca}^{2+}$  fluxes were measured using the scanning ion-selective electrode technique (SIET) as described previously (Holdaway-Clarke *et al.*, 1997) with small modifications in Xu-Yue company (Sci. & Tech. Co. Ltd, Beijing, China; www.xuyue.net).  $\text{Ca}^{2+}$ -selective microelectrodes with an external tip diameter of *c.* 3  $\mu\text{m}$  were manufactured and salinized with tributylchlorosilane, and the tips were backfilled with commercially available ion-selective cocktails (Calcium Ionophore I – Cocktail A, 21048; Fluka, Busch, Switzerland). The self-referencing vibrating probe oscillated with an excursion of 10  $\mu\text{m}$ , completing a whole cycle in *c.* 5.72 s. Extracellular  $\text{Ca}^{2+}$  fluxes at the tip of a pollen tube were measured by positioning the electrode tip on the normal to the tangent at the very tip and setting the direction of vibration to be parallel to the long axis of the pollen tube (Video S1). Pollen tubes selected for measurement were *c.* 100  $\mu\text{m}$  in length and were growing normally. All experiments were repeated three times, and the  $\text{Ca}^{2+}$  fluxes of at least 10 pollen tubes were measured in each treatment each time. Pollen tubes that showed stable fluctuations in the preliminary detection were selected for the subsequent net  $\text{Ca}^{2+}$  flux measurements with SNAP, cPTIO or L-NNA, and representative changes upon different treatments were plotted against time. Furthermore, the mean values for different treatments were calculated from at least five pollen tubes to illustrate the  $\text{Ca}^{2+}$  flux variations upon different pharmacological applications. The data obtained were analyzed using an Excel spreadsheet to convert data from the background-mV estimation of concentration and the microvolt-difference estimation of the local gradient into specific ion influx ( $\text{pmol cm}^{-2} \text{ s}^{-1}$ ) (Franklin-Tong *et al.*, 2002).

#### Fluorescence labeling of F-actin

Labeling of F-actin was performed as previously described with small modifications (Chen *et al.*, 2007). Samples were observed under CLSM with excitation at 488 nm and emission at 500–550 nm. All images were projected along the *z*-axis.

#### FM4-64 staining to analyze vesicle trafficking in the tube apex

Loading of cells with FM4-64 dye was generally achieved by direct application to the growing pollen tubes as described

previously with slight modifications (Chen *et al.*, 2007). The samples were excited at 514 nm with a 25-mW argon laser. Serial optical sections were performed every 20 s for *c.* 60 images 1 min after dye application until the fluorescence finally reached saturation, and the images were processed with CLSM 510 META software.

#### Fluorescent immunolabeling of pectins in the pollen tube cell wall

Immunolabeling of pectins in pollen tube cell walls was carried out according to Chen *et al.* (2007) with slight modifications. All the samples were excited at 488 nm under CLSM and emission signals were collected at 500–550 nm. Controls were prepared by omitting the primary antibody.

#### Fluorescence labeling of callose

Callose in the pollen tube cell wall was labeled with decolorized aniline blue as described by Chen *et al.* (2007). The stained samples were examined with differential interference contrast (DIC) followed by epifluorescence (ultraviolet excitation), and then photographed using a Zeiss Axioskop 40 microscope (excitation filter BP395-440; chromatic beam splitter FT460; barrier filter LP 470).

#### Fourier transform infrared (FTIR) analysis of the pollen tube walls

Pollen tubes were repeatedly washed with  $\text{ddH}_2\text{O}$  four times and then dried in a layer on a barium fluoride window (13 mm diameter  $\times$  2 mm). FTIR spectra were recorded on a Perkin-Elmer Cetus MAGNA 750 FTIR spectrometer (Nicolet Corp., Tokyo, Japan) equipped with a mercury–cadmium–telluride (MCT) detector, and the Perkin-Elmer Cetus microscope was interfaced to a personal computer. An area of *c.* 100  $\times$  100  $\mu\text{m}$  was selected for FTIR analysis. The acquisition parameters were 8  $\text{cm}^{-1}$  resolution, 128 co-added interferograms, and spectra were normalized to obtain relative absorbance (Chen *et al.*, 2007).

## Results

### Pollen tube growth and morphological observations

As shown in Tables 1–3, SNAP stimulated pollen germination and pollen tube growth in a dose-dependent manner (Table 1). By contrast, cPTIO and L-NNA significantly delayed pollen germination and pollen tube growth in a dose-dependent manner (Tables 2, 3). Furthermore, under control conditions, pollen tubes had a uniform diameter and a clear zone at the tip (Fig. S2a,e). However, pollen tube elongation was stimulated by 15  $\mu\text{M}$  SNAP and the morphology of SNAP-treated pollen tubes did not show significant changes (Fig. S2b,f). In contrast,

pollen tubes were shorter and many of them exhibited obvious abnormalities, including swollen tips, loss of the clear zone at the tube tips, and even bipolar growth, in the presence of 100  $\mu\text{M}$  cPTIO (Fig. S2c,g) or 45  $\mu\text{M}$  L-NNA (Fig. S2d,h) for 24 h.

### SNAP, cPTIO and L-NNA affect intracellular NO production

In the control, NO was distributed throughout nearly the entire tube in a compartmentalized fashion, but almost no fluorescence was detected in the tip region (Fig. 1a). In comparison, NO was distributed throughout almost the entire tube in cells treated with 100  $\mu\text{M}$  cPTIO or 45  $\mu\text{M}$  L-NNA, including the tip region (Fig. 1b,c), but fluorescence was weaker compared with that in control cells (Fig. 1b,c,e). In pollen tubes treated

with 15  $\mu\text{M}$  SNAP, significant fluorescence was detected almost along the entire tubes, except at the very tip (Fig. 1d,e).

### Effects of NO on the intracellular $\text{Ca}^{2+}$ gradient and extracellular $\text{Ca}^{2+}$ flux at the pollen tube tip

Pollen tubes grown under normal conditions exhibited the typical tip-to-base cytoplasmic  $\text{Ca}^{2+}$  concentration gradient (Fig. 2a); whereas pollen tubes treated with 100  $\mu\text{M}$  cPTIO showed a negligible cytosolic  $\text{Ca}^{2+}$  gradient (Fig. 2b). Similarly, treatment with 45  $\mu\text{M}$  L-NNA also led to a narrow cytosolic  $\text{Ca}^{2+}$  gradient from tip to base (Fig. 2c). However, pollen tubes exhibited a sharper tip-focused  $\text{Ca}^{2+}$  gradient after treatment with 15  $\mu\text{M}$  SNAP in comparison to that of control pollen tubes (Fig. 2d). Furthermore, the pollen tubes retained normal morphology and a well-characterized clear zone in the tip region after control injection, and recovered normal fountain-like cytoplasmic streaming (Video S2), indicating that injection did not affect pollen tube growth.

A consistent  $\text{Ca}^{2+}$  influx near the very tip and stable fluctuations were observed in normally growing pollen tubes within the first 360 s, and then 15  $\mu\text{M}$  SNAP, 100  $\mu\text{M}$  cPTIO or 45  $\mu\text{M}$  L-NNA was added to the controls.  $\text{Ca}^{2+}$  influx significantly increased after addition of 15  $\mu\text{M}$  SNAP, and then became relatively stable after *c.* 180 s (Fig. 3a). In addition, the range of influx in SNAP-treated pollen tubes was *c.* 77 to 130  $\text{pmol cm}^{-2} \text{s}^{-1}$  (with a mean value of  $100 \pm 5.7 \text{ pmol cm}^{-2} \text{s}^{-1}$ ;  $n = 15$ ), whereas the influx in controls ranged from *c.* 48 to 82  $\text{pmol cm}^{-2} \text{s}^{-1}$  (with a mean value of  $63 \pm 3.5 \text{ pmol cm}^{-2} \text{s}^{-1}$ ;

**Table 1** Effects of S-nitroso-N-acetylpenicillamine (SNAP) on pollen germination and mean tube length in *Pinus bungeana*

SNAP ( $\mu\text{mol l}^{-1}$ )	Germination percentage (%)	Pollen tube length ( $\mu\text{m}$ )		
		60 h	72 h	84 h
0	81.3 $\pm$ 3.12	75.6 $\pm$ 2.93	92.7 $\pm$ 4.17	102 $\pm$ 3.93
5	84.4 $\pm$ 2.58	74.9 $\pm$ 3.22	97.3 $\pm$ 3.79	110 $\pm$ 4.37
10	86.9 $\pm$ 3.02	75.1 $\pm$ 3.49	104 $\pm$ 4.68	117 $\pm$ 4.01
15	90.1 $\pm$ 2.76	74.7 $\pm$ 3.61	112 $\pm$ 5.22	124 $\pm$ 3.55

Only pollen tubes that were longer than the diameter of the pollen grain were considered to have germinated. Values are the mean  $\pm$  SD.

cPTIO ( $\mu\text{mol l}^{-1}$ )	Germination percentage (%)	Pollen tube length ( $\mu\text{m}$ )		
		60 h	72 h	84 h
0	82.7 $\pm$ 3.87	74.4 $\pm$ 3.44	93.1 $\pm$ 3.48	100 $\pm$ 4.55
50	67.9 $\pm$ 3.07	75.2 $\pm$ 2.91	88.9 $\pm$ 4.02	95.8 $\pm$ 4.29
100	48.7 $\pm$ 2.95	74.6 $\pm$ 3.65	85.2 $\pm$ 4.73	89.0 $\pm$ 3.12
150	45.3 $\pm$ 2.33	73.7 $\pm$ 2.87	80.3 $\pm$ 4.59	83.4 $\pm$ 3.51
200	0	74.1 $\pm$ 3.05	76.2 $\pm$ 3.88	78.7 $\pm$ 3.43

Only pollen tubes that were longer than the diameter of pollen grain were considered to have germinated. Values are the mean  $\pm$  SD.

L-NNA ( $\mu\text{mol l}^{-1}$ )	Germination percentage (%)	Pollen tube length ( $\mu\text{m}$ )		
		60 h	72 h	84 h
0	80.9 $\pm$ 3.30	74.9 $\pm$ 3.12	93.3 $\pm$ 4.16	104 $\pm$ 3.14
15	73.8 $\pm$ 2.77	75.5 $\pm$ 3.26	86.6 $\pm$ 3.64	95.3 $\pm$ 3.66
30	67.5 $\pm$ 3.15	74.8 $\pm$ 3.44	82.8 $\pm$ 4.08	88.9 $\pm$ 3.05
45	47.6 $\pm$ 2.06	73.7 $\pm$ 3.67	78.1 $\pm$ 4.96	82.5 $\pm$ 4.81
60	0	74.3 $\pm$ 4.01	75.9 $\pm$ 5.19	77.3 $\pm$ 4.73

Only pollen tubes that were longer than the diameter of the pollen grain were considered to have germinated. Values are the mean  $\pm$  SD.

**Table 2** Effects of 2-(4-carboxyphenyl)-4, 4, 5, 5-tetramethylimidazole-1-oxyl-3-oxide (cPTIO) on pollen germination and mean tube length in *Pinus bungeana*

**Table 3** Effects of  $N_{\omega}$ -nitro-L-arginine (L-NNA) on pollen germination and mean tube length in *Pinus bungeana*

**Fig. 1** Effects of 2-(4-carboxyphenyl)-4, 4, 5, 5-tetramethylimidazole-1-oxyl-3-oxide (cPTIO),  $N_{\omega}$ -nitro-L-arginine (L-NNA) and S-nitroso-N-acetylpenicillamine (SNAP) on intracellular nitric oxide (NO) production in *Pinus bungeana* pollen tubes. Bar, 20  $\mu\text{m}$ . (a) In control pollen tubes cultured for 84 h, the fluorescence was distributed throughout nearly the entire tube, except in the tip region. (b) The fluorescence was distributed throughout nearly the entire tube after treatment with 100  $\mu\text{M}$  cPTIO for 24 h. (c) The fluorescence was distributed throughout nearly the entire tube upon treatment with 45  $\mu\text{M}$  L-NNA for 24 h. (d) In pollen tubes treated with 15  $\mu\text{M}$  SNAP for 24 h, the fluorescence was distributed throughout nearly the entire tube, but almost no fluorescence was detected in the tip region. (e) The relative fluorescence intensities were measured using IMAGEJ software. At least 50 pollen tubes were monitored in each of five replicates and corresponding mean fluorescence intensities were calculated.

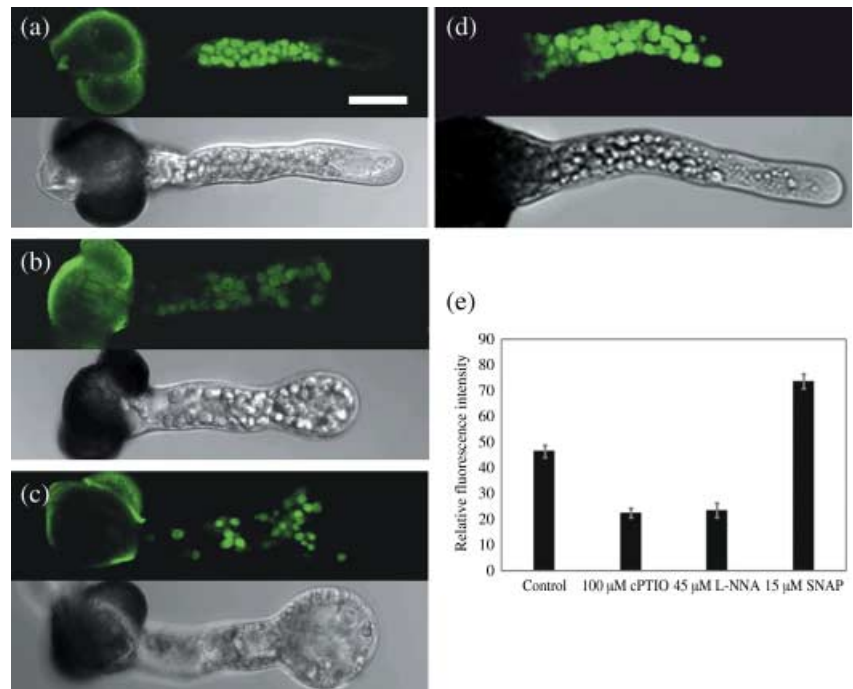
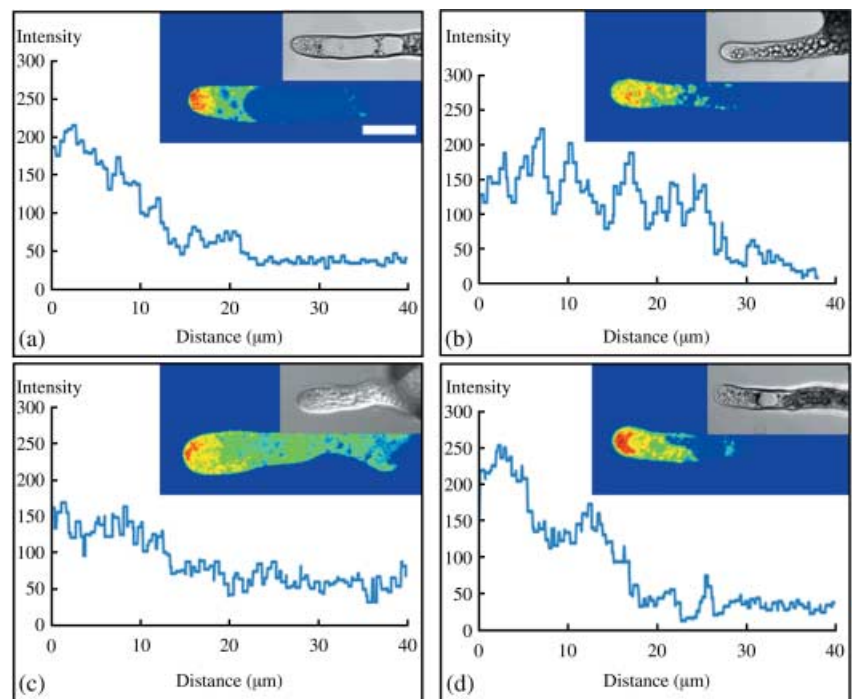


**Fig. 2** Changes in the tip-focused  $\text{Ca}^{2+}$  gradient in *Pinus bungeana* pollen tubes after treatment with 2-(4-carboxyphenyl)-4, 4, 5, 5-tetramethylimidazole-1-oxyl-3-oxide (cPTIO),  $N_{\omega}$ -nitro-L-arginine (L-NNA) and S-nitroso-N-acetylpenicillamine (SNAP). The fluorescence intensities were analyzed by CLSM 510 META software. Corresponding bright field images are shown at a reduced size. Bar, 20  $\mu\text{m}$ . (a) Control pollen tubes exhibited the typical tip-focused cytosolic  $\text{Ca}^{2+}$  concentration ( $[\text{Ca}^{2+}]_{\text{cyt}}$ ) gradient. (b) Pollen tubes treated with 100  $\mu\text{M}$  cPTIO showed a disrupted  $[\text{Ca}^{2+}]_{\text{cyt}}$  gradient. (c) Pollen tubes treated with 45  $\mu\text{M}$  L-NNA exhibited a negligible  $[\text{Ca}^{2+}]_{\text{cyt}}$  gradient. (d) Pollen tubes treated with 15  $\mu\text{M}$  SNAP showed a sharper  $[\text{Ca}^{2+}]_{\text{cyt}}$  gradient.



$n = 15$ ) (Fig. 3a). By contrast, treatment with 100  $\mu\text{M}$  cPTIO led to a decrease in  $\text{Ca}^{2+}$  influx and the amplitude of influx ranged from 10 to 30  $\text{pmol cm}^{-2} \text{s}^{-1}$  (with a mean value of  $22 \pm 2.3 \text{ pmol cm}^{-2} \text{s}^{-1}$ ;  $n = 15$ ), which was narrower than that of control pollen tubes (ranging from 41 to 78  $\text{pmol cm}^{-2} \text{s}^{-1}$ ; the mean value was  $59 \pm 2.7 \text{ pmol cm}^{-2} \text{s}^{-1}$ ;  $n = 15$ ) (Fig. 3b).

Similarly, the  $\text{Ca}^{2+}$  influx dramatically decreased upon treatment with 45  $\mu\text{M}$  L-NNA and also showed a narrow flux range (from 15 to 36  $\text{pmol cm}^{-2} \text{s}^{-1}$ ; the mean value was  $27 \pm 3.1 \text{ pmol cm}^{-2} \text{s}^{-1}$ ;  $n = 15$ ) in comparison to that of control pollen tubes (from 49 to 80  $\text{pmol cm}^{-2} \text{s}^{-1}$ ; the mean value was  $64 \pm 3.2 \text{ pmol cm}^{-2} \text{s}^{-1}$ ;  $n = 15$ ) (Fig. 3c).

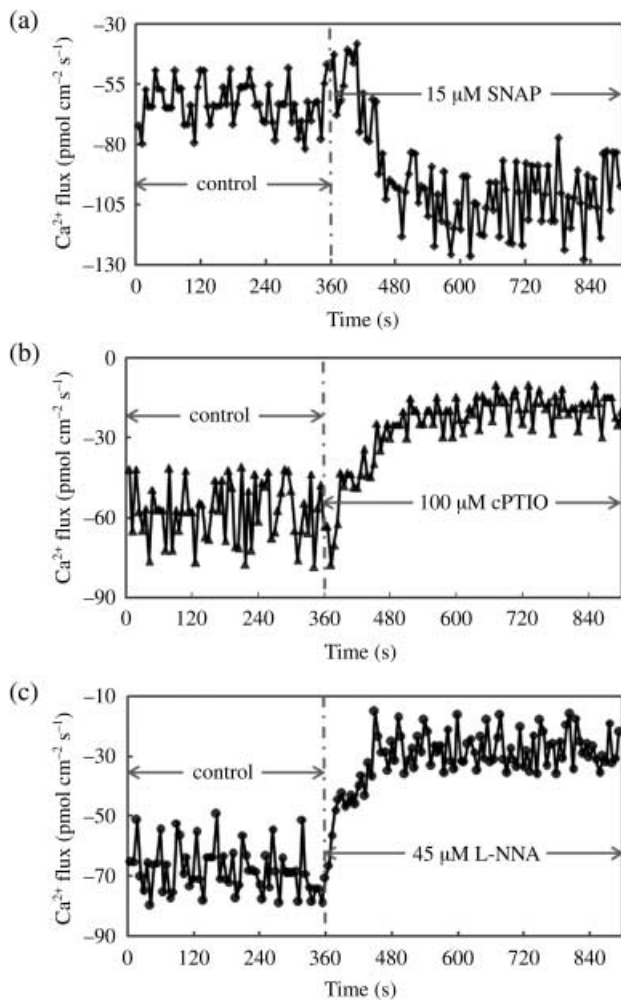


**Fig. 3** Extracellular  $\text{Ca}^{2+}$  influx at the pollen tube tips of *Pinus bungeana* before and after applications of S-nitroso-N-acetylpenicillamine (SNAP), 2-(4-carboxyphenyl)-4, 4, 5, 5-tetramethylimidazole-1-oxyl-3-oxide (cPTIO) and  $N_{\omega}$ -nitro-L-arginine (L-NNA). All of the experiments were repeated three times and the  $\text{Ca}^{2+}$  fluxes of at least 10 pollen tubes were measured in each treatment at each time. Pollen tubes that showed stable fluctuations in the preliminary detection were selected for the subsequent net  $\text{Ca}^{2+}$  flux measurements. SNAP, L-NNA or cPTIO was added after 360 s. (a) A consistent  $\text{Ca}^{2+}$  influx (ranging from 48 to 82  $\text{pmol cm}^{-2} \text{s}^{-1}$ , with a mean value of  $63 \pm 3.5 \text{ pmol cm}^{-2} \text{s}^{-1}$ ;  $n = 15$ ) was detected at the tip of control pollen tubes in the first 360 s, and 15  $\mu\text{M}$  SNAP treatment led to a dramatic increase in  $\text{Ca}^{2+}$  influx in the next 180 s and then the influx fluctuation (ranging from 77 to 130  $\text{pmol cm}^{-2} \text{s}^{-1}$ , with a mean value of  $100 \pm 5.7 \text{ pmol cm}^{-2} \text{s}^{-1}$ ;  $n = 15$ ) reached a plateau. (b) A consistent  $\text{Ca}^{2+}$  influx, ranging from 41 to 78  $\text{pmol cm}^{-2} \text{s}^{-1}$  (with a mean value of  $59 \pm 2.7 \text{ pmol cm}^{-2} \text{s}^{-1}$ ;  $n = 15$ ), was detected in the first 360 s; subsequently, the application of 100  $\mu\text{M}$  cPTIO resulted in a marked decrease in  $\text{Ca}^{2+}$  influx within the next 180 s and then the influx fluctuation reached a lower stable level, ranging between 10 and 30  $\text{pmol cm}^{-2} \text{s}^{-1}$  (with a mean value of  $22 \pm 2.3 \text{ pmol cm}^{-2} \text{s}^{-1}$ ;  $n = 15$ ). (c) A consistent  $\text{Ca}^{2+}$  influx, ranging from 49 to 80  $\text{pmol cm}^{-2} \text{s}^{-1}$  (with a mean value of  $64 \pm 3.2 \text{ pmol cm}^{-2} \text{s}^{-1}$ ;  $n = 15$ ), was detected within 360 s. It was significantly reduced upon 45  $\mu\text{M}$  L-NNA treatment in the next 180 s and then a lower plateau of influx fluctuation (ranging from 15 to 36  $\text{pmol cm}^{-2} \text{s}^{-1}$ , with a mean value of  $27 \pm 3.1 \text{ pmol cm}^{-2} \text{s}^{-1}$ ;  $n = 15$ ) was detected.

### Stimulatory effects of L-NNA on actin polymerization and organization

Microscopic analysis revealed that the AFs were distributed throughout the entire pollen tube in a net axial array that was largely parallel to the direction of elongation in control tubes, except in the elongation tip region (Fig. 4a), where only a dense array of fine AFs was detected (Fig. 4b). Furthermore, a net axial array of AFs parallel to the direction of elongation was also observed in pollen tubes treated with 15  $\mu\text{M}$  SNAP (Fig. 4c), but AFs at the tips of pollen tubes were depolymerized and even thinner (Fig. 4c,d). By contrast, thick actin bundles were detected along the entire length of pollen tubes treated with 100  $\mu\text{M}$  cPTIO (Fig. 4e) or 45  $\mu\text{M}$  L-NNA (Fig. 4g). Moreover, these thick actin bundles extended into the extreme tip of cPTIO- (Fig. 4f) or L-NNA-treated (Fig. 4h) pollen tubes.

### FM4-64 staining following NO manipulation

Uptake of FM4-64 into pollen tubes was strictly time-dependent (Fig. 5). The plasma membrane was stained immediately after application of the dye. Bright spherical structures were observed in apical and subapical regions within 5 min (Fig. 5a). A typical reverse V-like staining pattern became apparent after *c.* 16 min (Fig. 5a). In SNAP-treated pollen tubes, the same staining pattern was observed in the cytoplasm within *c.* 10 min (Fig. 5b).

By contrast, a completely distinct staining pattern was observed in the cytoplasm of L-NNA-treated pollen tubes (Fig. 5c,d). In pollen tubes with a significantly swollen tip, FM dye uptake took place all along these swollen regions (Fig. 5c). In addition, FM dye uptake into the L-NNA-treated pollen tubes without balloon tips took place not only in the apical and subapical regions but also in the basal part of the pollen tubes, and finally the fluorescence was distributed almost evenly throughout the pollen tube (Fig. 5d). Furthermore, the uptake of FM4-64 in L-NNA-treated cells took *c.* 20 min, which was longer than in the controls (Fig. 5c,d), indicating possible variations in either cell wall construction or the pattern of dye internalization.

### Effects of L-NNA on pectin distribution

In control pollen tubes, the distribution of JIM5-reactive (de-esterified) pectins was relatively uniform, except at the tip (Fig. 6a), whereas localization of JIM7-reactive (esterified) pectins was limited to the very tip of the growing tubes (Fig. 6c). By contrast, de-esterified pectins were detected across the entire surface of the pollen tubes treated with 45  $\mu\text{M}$  L-NNA, including the tips (Fig. 6b), and esterified pectins were detected only in basal sites (Fig. 6d).

### Effects of L-NNA on callose deposition

Callose was distributed almost evenly along the long tube shank in control pollen tubes, as shown by aniline blue staining

**Fig. 4** Reorganization of the actin cytoskeleton in pollen tubes of *Pinus bungeana* in response to various compounds. Corresponding bright field images were shown at a reduced size. Bar, 20  $\mu\text{m}$ . (a) Control pollen tubes cultured for 84 h, showing that actin filaments (AFs) were distributed throughout the whole pollen tube in a net axial array mainly parallel to the direction of elongation. (b) Amplified image of the control pollen tube tip, showing that only a dense array of fine actin could be found in the tip region of control pollen tubes. (c) A pollen tube treated with 15  $\mu\text{M}$  S-nitroso-N-acetylpenicillamine (SNAP) for 24 h, showing a net axial array of AFs parallel to the direction of elongation. (d) Amplified image of the tip region in pollen tubes treated with 15  $\mu\text{M}$  SNAP, showing disorganized actin fragments in the tip region. (e) A pollen tube treated with 100  $\mu\text{M}$  2-(4-carboxyphenyl)-4, 4, 5, 5-tetramethylimidazoline-1-oxyl-3-oxide (cPTIO) for 24 h, showing that the actin cytoskeleton polymerized into thick actin bundles which existed at the tip of the pollen tube. (f) An amplified image of the tip region in pollen tubes treated with 100  $\mu\text{M}$  cPTIO, showing that thick actin bundles extended into the very tip of the pollen tube. (g) A pollen tube treated with 45  $\mu\text{M}$   $N_{\omega}$ -nitro-L-arginine (L-NNA) for 24 h, showing that the actin cytoskeleton polymerized into thick actin bundles which even extended into the tip region of the pollen tube. (h) An amplified image of the tip region in pollen tubes treated with 45  $\mu\text{M}$  L-NNA, showing that actin bundles existed in the tip of the pollen tube.

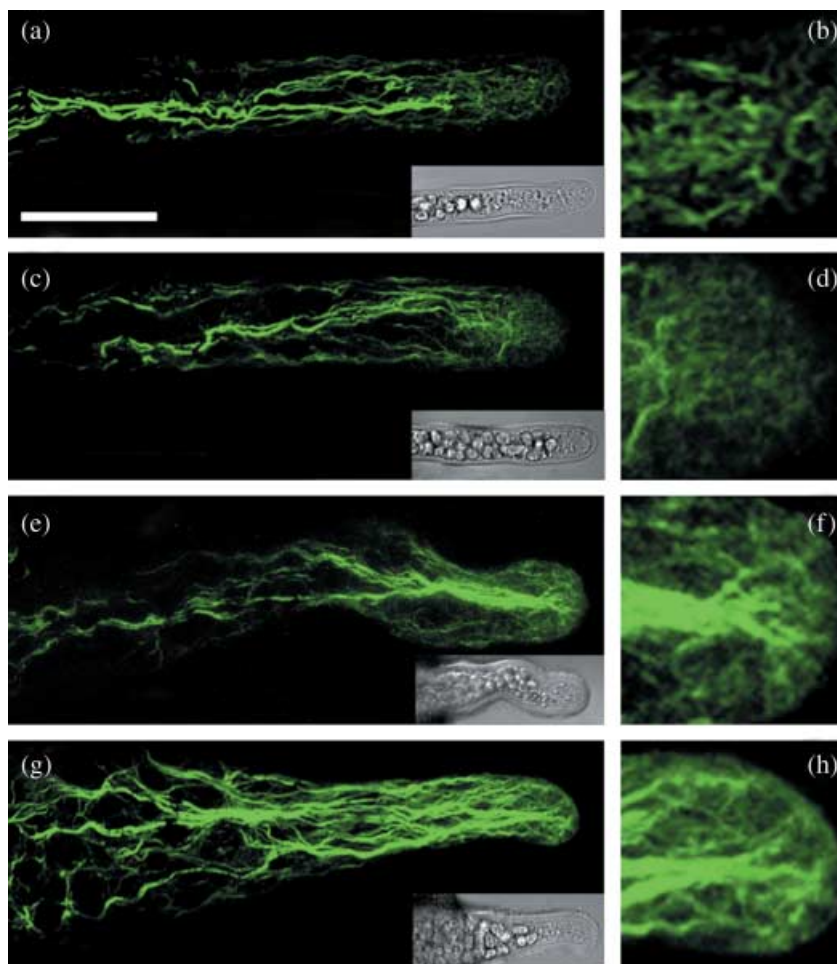


(Fig. 6e). By contrast, strong fluorescence was detected in the tip region of the pollen tubes treated with 45  $\mu\text{M}$  L-NNA, suggesting enhanced callose synthesis and deposition at the tip in response to L-NNA treatment (Fig. 6f).

#### FTIR analysis of wall components in pollen tubes

Typical FTIR spectra obtained from the tip region of control and 15  $\mu\text{M}$  SNAP- or 45  $\mu\text{M}$  L-NNA-treated pollen tubes are shown in Fig. 7(a). A saturated ester peak (representative of esterified pectins) was detected at 1743  $\text{cm}^{-1}$  (Morikawa *et al.*, 1978). The carboxylic acid peak (representative of de-esterified pectins) at *c.* 1419  $\text{cm}^{-1}$  (Morikawa *et al.*, 1978) was not distinct. To identify possible changes in pectins, differential spectra were generated by the digital subtraction of spectra for the tip region of control pollen tubes from those of 15  $\mu\text{M}$  SNAP- or 45  $\mu\text{M}$  L-NNA-treated pollen tubes. Based on these spectra, a carboxylic acid peak with a negative value appeared at *c.* 1419  $\text{cm}^{-1}$ , and a saturated ester peak at *c.* 1743  $\text{cm}^{-1}$  exhibited increased absorbance intensity (Fig. 7b), indicating that exposure to 15  $\mu\text{M}$  SNAP lead to decrease in the de-esterified pectin and increase in the esterified pectin content. By contrast,

treatment with 45  $\mu\text{M}$  L-NNA resulted in an increase in de-esterified pectin content and a decrease in esterified pectin content (Fig. 7c).

#### Discussion

In recent years, NO has emerged as an important endogenous signaling molecule in plants with regulatory roles in many developmental and physiological processes, including tip growth (Prado *et al.*, 2008). Recent *in vitro* studies have indicated that, as lily pollen tubes move into the NO gradient produced by SNAP, their growth is reduced or abrogated while the pollen tube reorients, and is then subsequently resumed (Prado *et al.*, 2004). Our data show that pollen tube growth is stimulated by SNAP in a dose-dependent manner, while cPTIO and L-NNA inhibit pollen germination and pollen tube growth, accompanied by significant morphological alterations, indicating that cPTIO and L-NNA inhibit pollen germination and tube elongation in a dose-dependent manner, whereas He *et al.* (2007) reported that cPTIO and L-NAME (a NOS inhibitor) had no effect on pollen germination and tube growth in *P. tomentosa*. These differences in sensitivity to NO-modulating drugs may

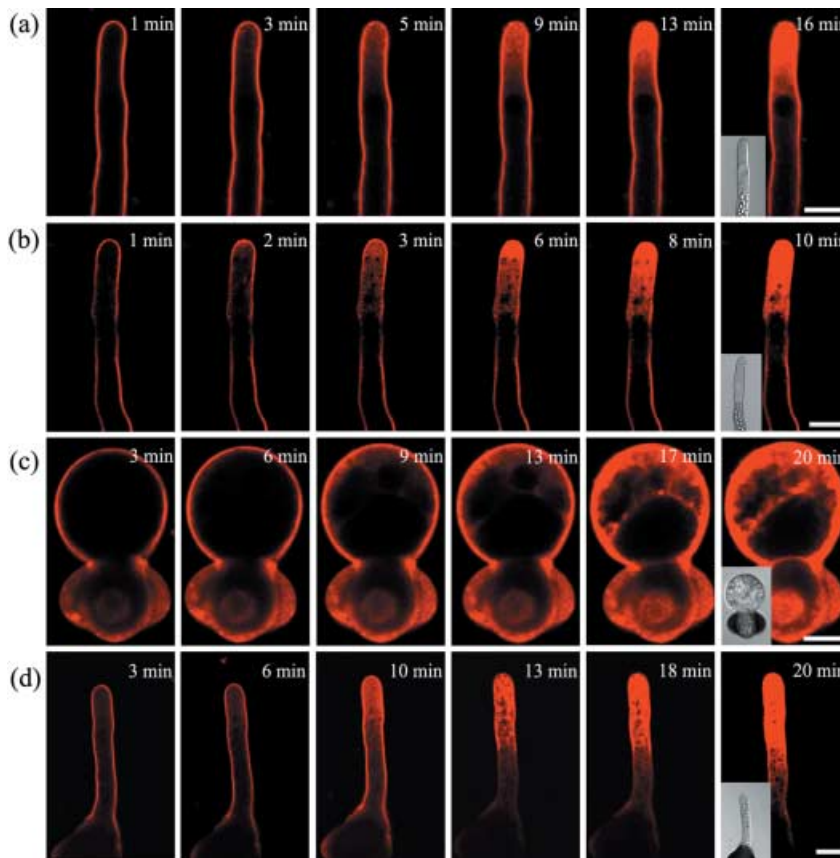


**Fig. 5** Time course of FM4-64 uptake in pollen tubes of *Pinus bungeana*. Corresponding bright field images are shown at a reduced size. Bar, 20  $\mu\text{m}$ . (a) Uptake of FM4-64 into the control pollen tube followed a strict time course and dye uptake took place in the apical and subapical regions. A characteristic pattern of FM4-64 was produced within c. 16 min. (b) FM4-64 staining of a pollen tube treated with 15  $\mu\text{M}$  S-nitroso-N-acetylpenicillamine (SNAP). FM4-64 internalization took place in the apical and subapical regions. Dye uptake followed a strict time course and saturation was reached within c. 10 min. (c) FM4-64 staining of a 45  $\mu\text{M}$   $N_{\text{o}}$ -nitro-L-arginine (L-NNA)-treated pollen tube with a significant balloon tip. The internalization of FM dye took place along the entire swollen region. Saturation of the signal was detected within c. 20 min. (d) FM4-64 staining of a 45  $\mu\text{M}$  L-NNA-treated pollen tube without a significant balloon tip. FM dye uptake took place not only in the apical and subapical regions but also in the basal part of the pollen tube. The dye was evenly distributed in the pollen tube and saturation of the signal was detected within c. 20 min.

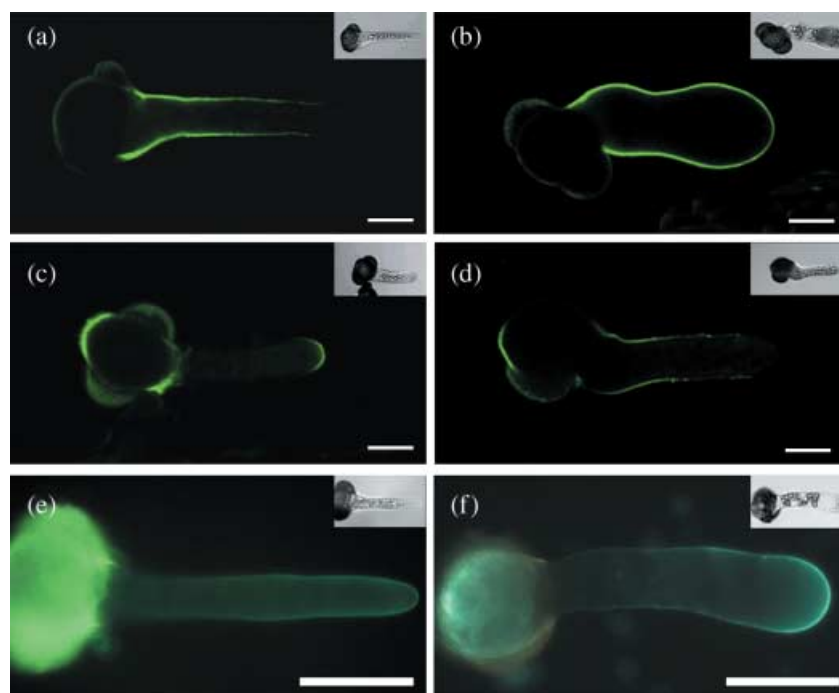
result in the general differences in responsiveness to SNAP, cPTIO or L-NNA that have been observed in several plant species. These differences may come about because *P. bungeana* pollen tubes grow far more slowly than angiosperm pollen tubes.

The involvement of NO in tip growth has been investigated using pharmacological agents to alter endogenous NO concentrations (Prado *et al.*, 2004; He *et al.*, 2007; Salmi *et al.*, 2007). In the present study, SNAP was selected as the NO donor instead of sodium nitroprusside (SNP), because application of SNP as an NO donor has side effects (Planchet & Kaiser, 2006; Schröder, 2006). The results showed that endogenously generated NO was almost absent at the tip of control pollen tubes but was at higher concentrations behind the clear zone of the tip region, which are in accordance with the findings of Prado *et al.* (2004) in lily pollen tubes. These results indicate that an appropriate concentration of NO behind the tip region is a positive growth regulator, at least in gymnosperm pollen tubes. NO was found in the tip region of pollen tubes treated with cPTIO or L-NNA, because cPTIO or L-NNA disrupted the clear zone of pollen tubes. This result might give rise to potential changes in the regulation of  $\text{Ca}^{2+}$  influx as indicated by the results from the net  $\text{Ca}^{2+}$  flux measurements.

$\text{Ca}^{2+}$  serves as a second messenger in a variety of plant physiological processes. There is a close coupling between the intracellular tip-focused  $\text{Ca}^{2+}$  gradient, extracellular tip-

directed  $\text{Ca}^{2+}$  influx, and elongation of the pollen tube (Holdaway-Clarke & Hepler, 2003). Increasing evidence suggests that there is a connection between NO and  $\text{Ca}^{2+}$  signaling pathways. Pharmacological and biochemical studies have shown that NO signaling in plants is mediated by cGMP (Prado *et al.*, 2004; Salmi *et al.*, 2007) and cyclic nucleotide-gated ion channels (CNGCs), which are permeable to both monovalent and divalent cations (typically  $\text{K}^+$ ,  $\text{Na}^+$ , and  $\text{Ca}^{2+}$ ) and are directly activated by cGMP and/or cAMP (Lanteri *et al.*, 2006). Recently, Prado *et al.* (2008) reported that activation of  $\text{Ca}^{2+}$  influx in pollen tubes partially eliminated the balloon tips induced by cPTIO, indicating that a putative NO-cGMP signaling pathway is dependent on  $\text{Ca}^{2+}$  signaling, through effects on cytosolic  $\text{Ca}^{2+}$  concentrations during NO-induced pollen tube reorientation. On the basis of the results obtained regarding the  $\text{Ca}^{2+}$  gradient and  $\text{Ca}^{2+}$  influx in the present study, we conclude that NO regulates the cytoplasmic  $\text{Ca}^{2+}$  gradient largely by mediating  $\text{Ca}^{2+}$  influx, which is probably dependent on cGMP-activated channels in pollen tubes (Frietsch *et al.*, 2007), to regulate pollen tube development. Furthermore, the 2-fold tip-focused  $\text{Ca}^{2+}$  gradient in conifer pollen tubes is much lower than the 10-fold gradient within 20  $\mu\text{m}$  in angiosperm pollen tubes (Lazzaro *et al.*, 2005). Considering the slow growth rate of gymnosperm pollen tubes in comparison to angiosperm pollen tubes

**Fig. 6** Effects of *N*<sub>ω</sub>-nitro-L-arginine (L-NNA) on the distribution of de-esterified pectins, esterified pectins and callose in the pollen tube cell wall of *Pinus bungeana*. Corresponding bright field images are shown at a reduced size. Bar, 20 μm. (a) JIM5 labeling of control pollen tubes observed by CLSM, showing that strong fluorescence occurred along the entire pollen tube wall except for the tip region. (b) JIM5 labeling of pollen tubes treated with 45 μM L-NNA observed by CLSM, showing that strong fluorescence occurred along the entire pollen tube wall, including the tip region. (c) JIM7 labeling of a control pollen tube observed by CLSM, showing that the esterified pectins localized in the tip region of the pollen tube. (d) JIM7 labeling of pollen tubes treated with 45 μM L-NNA observed by CLSM, showing that esterified pectins accumulated in the basal part of the pollen tube and were not detected in the tip region. (e) A control pollen tube labeled with aniline blue observed using a Zeiss Axioskop 40 microscope. The fluorescence was distributed evenly along the shank of the pollen tube. (f) A pollen tube treated with 45 μM L-NNA labeled with aniline blue was observed using a Zeiss Axioskop 40 microscope, showing strong fluorescence deposited in the tip region.



and the previous results showing that the  $\text{Ca}^{2+}$  gradient was related to the polarized growth rate (Silverman-Gavrila & Lew, 2003; Cárdenas *et al.*, 2008), we assume that the increase in growth rate upon SNAP treatment may partly result from the greater steepness of the tip-focused  $\text{Ca}^{2+}$  gradient in comparison to that of control pollen tubes, and that the slower growth rate of the pollen tube in response to cPTIO/L-NNA probably results from the lower steepness of the  $\text{Ca}^{2+}$  gradient.

In addition, accumulating evidence indicates that AFs control cytoplasmic streaming and hence the transport of secretory vesicles, and that actin polymerization itself also contributes to pollen tube growth (Chen *et al.*, 2007). The dynamic state of the cytoskeleton is controlled via numerous regulatory factors, including several actin-binding proteins activated in response to  $\text{Ca}^{2+}$  (Cárdenas *et al.*, 2008). Our results show that NO stimulation induced depolymerization of F-actin accompanied by a sharper  $\text{Ca}^{2+}$  gradient, and a reduction of NO induced the polymerization of F-actin in the pollen tube tip region accompanied by a negligible  $\text{Ca}^{2+}$  gradient. This suggests that F-actin organization in the tip region of pollen tubes sensitive to NO is partly dependent on the  $\text{Ca}^{2+}$  gradient during NO signaling in pollen tubes. Furthermore, the effects of cPTIO and L-NNA are reminiscent of previous studies which reported that polymerization of actin in pollen tube tips blocks tube growth (Cárdenas *et al.*, 2005). Time-lapse images of L-NNA-treated pollen tubes showed a distinct FM dye staining pattern from that of controls, suggesting that vesicular trafficking was perturbed by the reduction of NO. This is consistent with a

previous report showing that FM is a marker for polar growth (Camacho & Malhó, 2003). Interestingly, internalization of the dye was faster in SNAP-treated cells and slower in L-NNA-treated cells than in control cells. This is supported by results obtained by Lowenstein (2007) showing that NO accelerates endocytosis in cardiovascular cells. Taking these findings together, we speculate that NO stimulates endocytosis, indicating that changes in cell wall modeling may be partly dependent on the polymerization status of F-actin in pollen tubes.

The dynamic balance between cell wall extensibility and rigidity is another key factor that regulates tip growth in pollen tubes (Rockel *et al.*, 2008). Immunolabeling with JIM5 and JIM7 showed that de-esterified pectins along the longitudinal axis seemed to decline gradually from the distal end towards the tube tip, whereas esterified pectins were present only in the tube tip region in control pollen tubes. This is consistent with data showing that the gradient in cell wall composition from apical esterified to distal de-esterified pectins, which is correlated with an increase in the degree of cell wall rigidity and a decrease in visco-elasticity, influences pollen tube growth and architecture (Parre & Geitmann, 2005). Compared with the controls, de-esterified pectins accumulated whereas esterified pectins decreased in concentration or disappeared completely in the tip region of L-NNA-treated pollen tubes. We propose that the conversion of esterified pectins to de-esterified pectins and/or the biosynthesis of esterified pectins is under the control of NO, and that the reduction in NO leads to excess wall rigidity at the tip of the pollen tube, which may partly account for the inhibition of pollen tube elongation in the presence of L-NNA.

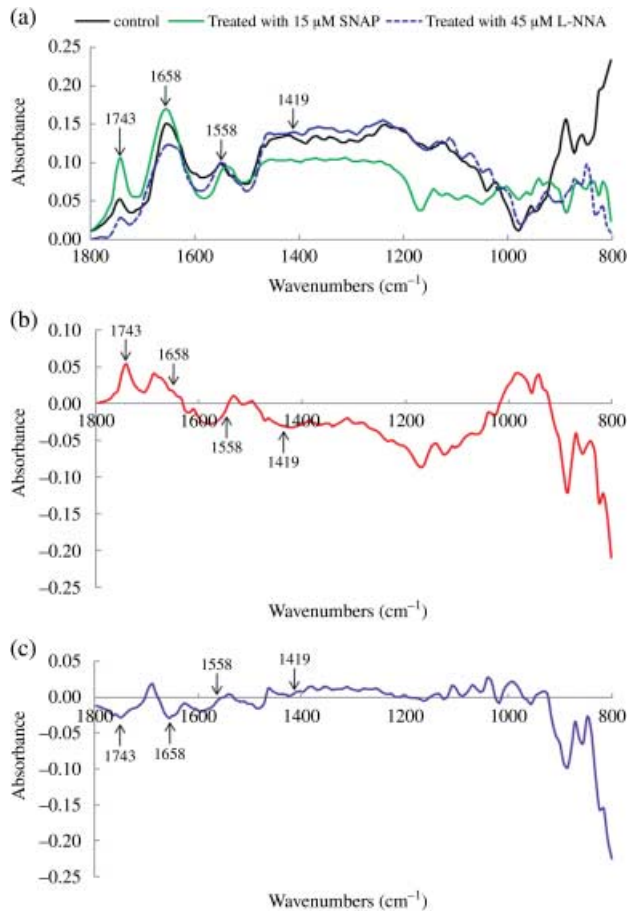


**Fig. 7** Fourier transform infrared microspectroscopic (FTIR) spectra obtained from the tip regions of pollen tubes of *Pinus bungeana*. (a) FTIR spectra obtained from the tip regions of control pollen tubes and pollen tubes treated with 15  $\mu\text{M}$  *S*-nitroso-*N*-acetylpenicillamine (SNAP) or 45  $\mu\text{M}$  *N*<sub>ω</sub>-nitro-*L*-arginine (L-NNA). An esterified pectin peak was detected at 1743  $\text{cm}^{-1}$  and de-esterified peaks absorbed at 1419  $\text{cm}^{-1}$ . (b) The differential spectrum generated by digital subtraction of the control spectra from the spectra of SNAP-treated tube walls showed the enhanced deposition of esterified pectins as well as a decrease in de-esterified pectin deposition in SNAP-treated pollen tubes. (c) The differential spectrum generated by digital subtraction of the control spectra from the spectra of L-NNA-treated tube walls showed a decrease in esterified pectins and an increase in de-esterified pectins in the apical region of pollen tubes after treatment with L-NNA.

In addition, both types of pectin are sensitive to NO inhibitors because they are transported via either Golgi apparatus-based (esterified pectins) constitutive secretion (Geitmann *et al.*, 1996) or endosomal recycling (de-esterified pectins) pathways (Baluška *et al.*, 2002). Furthermore, in the present study, callose was deposited in the apical region of L-NNA-treated pollen tubes, indicating that NO spatially and developmentally mediates the synthesis and distribution of callose, thereby contributing to the mechanical properties of the cell wall and thus affecting pollen tube growth. This result confirms the findings that massive accumulation of callose in pollen tube tips is an important

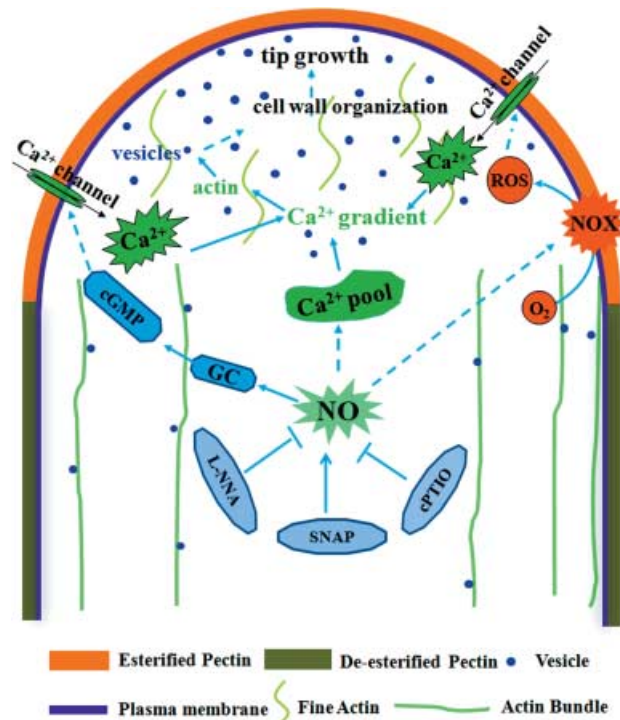


**Fig. 8** Hypothetical model showing the potential nitric oxide (NO) signaling events that lead to pollen tube tip growth. This simplified model was based on the models in root hairs proposed by Šamaj *et al.* (2004) and Lanteri *et al.* (2006). NO induces an increase in cytosolic  $\text{Ca}^{2+}$  concentration ( $[\text{Ca}^{2+}]_{\text{cyt}}$ ) through the regulation of both the influx of  $\text{Ca}^{2+}$  from the extracellular space (via  $\text{Ca}^{2+}$  channels in the plasma membrane) and the release of  $\text{Ca}^{2+}$  from intracellular stores. As a consequence, the actin cytoskeleton is remodeled and vesicle trafficking is activated, resulting in cell wall construction. Together, these pathways lead to tip growth. Black arrows indicate the links established in the induction of pollen tube development; broken arrows represent indirect or still undescribed pathways in pollen tube tip growth. GC, guanylyl cyclase; cGMP, cyclic guanosine monophosphate; NOX, NADPH oxidase; NOS, nitric oxide synthase;  $\perp$ , inhibition.

manifestation of abnormally growing tubes (Chen *et al.*, 2007) and a common indicator of incompatible pollen (Guyon *et al.*, 2004).

FTIR analyses showed distinct peaks corresponding to saturated esters (1743  $\text{cm}^{-1}$ ) and other polysaccharides (1200–900  $\text{cm}^{-1}$ ) in control pollen tubes. However, the saturated ester peak was relatively weak in inhibitor-treated tubes and relatively strong in donor-treated tubes. Peaks designated as pectins were observed in a difference spectrum, showing that there were fewer esterified pectins in the inhibitor-treated pollen tube tips than in the control tube tips and that there were more esterified pectins in the donor-treated tube tips. The FTIR results suggest that the NO signaling pathway significantly influences deposition of cell wall components such as carboxylic acids and pectins in the pollen tubes, further confirming the results obtained by immunolabeling with JIM5/JIM7.

In summary, our investigation into the effects of SNAP, cPTIO and L-NNA on *P. bungeana* pollen tubes provides a more global view of the role of NO in polarized tip growth in pollen tubes. We found that NO promotes extracellular Ca<sup>2+</sup> influx, which may play a role in the maintenance of the tip-focused Ca<sup>2+</sup> gradient and which may alter AF organization. The resulting differences in vesicle trafficking and cell wall construction lead to variations in tip growth (Fig. 8). This study produced two novel findings. Firstly, NO is indispensable for maintenance of the typical tip-focused cytosolic Ca<sup>2+</sup> concentration gradient, partially through extracellular Ca<sup>2+</sup> influx, in *P. bungeana* pollen tubes. Secondly, inhibitor treatment can cause changes in the main cell wall components of pollen tubes, such as pectins and callose, especially in the apical region. This combined cytological and biochemical study provides new insights into the multifaceted mechanistic framework for the functions of NO in polarized tip growth of pollen tubes.

## Acknowledgements

This work was funded by the National Key Basic Research Program (2009CB119105) from MOST, the Knowledge Innovation Program of the Chinese Academy of Sciences, Grant No. KJJCX2-YW-L08 and a key project from NSFC (30730009). We are indebted to Professor Yuan Ming and Professor Ren Hai-Yun for their expert advice concerning the microinjection.

## References

- Baluška F, Hlavacka A, Šamaj J, Palme K, Robinson DG, Matoh T, McCurdy DW, Menzel D, Volkmann D. 2002. F-actin-dependent endocytosis of cell wall pectins in meristematic root cells. Insights from brefeldin A-induced compartments. *Plant Physiology* 130: 422–431.
- Beligni MV, Lamattina L. 2000. Nitric oxide stimulates seed germination and de-etiolation, and inhibits hypocotyl elongation, three light-inducible responses in plants. *Planta* 210: 215–221.
- Camacho L, Malhó R. 2003. Endo/exocytosis in the pollen tube apex is differentially regulated by Ca<sup>2+</sup> and GTPases. *Journal of Experimental Botany* 54: 83–92.
- Cárdenas L, Lovy-Wheeler A, Kunkel JG, Hepler, PK. 2005. Actin polymerization promotes the reversal of streaming in the apex of pollen tubes. *Cell Motility and Cytoskeleton* 61: 112–127.
- Cárdenas L, Lovy-Wheeler A, Kunkel JG, Hepler PK. 2008. Pollen tube growth oscillations and intracellular calcium levels are reversibly modulated by actin polymerization. *Plant Physiology* 146: 1611–1621.
- Chen T, Teng N, Wu X, Wang Y, Tang W, Šamaj J, Baluška F, Lin J. 2007. Disruption of actin filaments by latrunculin B affects cell wall construction in *Picea meyeri* pollen tube by disturbing vesicle trafficking. *Plant and Cell Physiology* 48: 19–30.
- Courtois C, Besson A, Dahan J, Bourque S, Dobrowolska G, Pugin A, Wendehenne D. 2008. Nitric oxide signalling in plants: interplays with Ca<sup>2+</sup> and protein kinases. *Journal of Experimental Botany* 59: 155–163.
- Franklin-Tong VE, Holdaway-Clarke TL, Straatman KR, Kunkel JG, Hepler PK. 2002. Involvement of extracellular calcium influx in the self-incompatibility response of *Papaver rhoeas*. *The Plant Journal* 29: 333–345.
- Frietsch S, Wang YF, Sladek C, Poulsen LR, Romanowsky SM, Schroeder JI, Harper JF. 2007. A cyclic nucleotide-gated channel is essential for polarized tip growth of pollen. *Proceedings of the National Academy of Sciences, USA* 104: 14531–14536.
- Geitmann A, Wojciechowicz K, Cresti M. 1996. Inhibition of intracellular pectin transport in pollen tube by monensin, brefeldin A and cytochalasin D. *Botanica Acta* 109: 373–381.
- Guo FQ, Crawford NM. 2005. Arabidopsis nitric oxide synthase 1 is targeted to mitochondria and protects against oxidative damage and dark-induced senescence. *Plant Cell* 17: 3436–3450.
- Guyon V, Tang WH, Monti MM, Raiola A, Lorenzo GD, McCormick S, Taylor LP. 2004. Antisense phenotypes reveal a role for SHY, a pollen-specific leucine-rich repeat protein, in pollen tube growth. *Plant Journal* 39: 643–654.
- He JM, Bai XL, Wang RB, Cao B, She XP. 2007. The involvement of nitric oxide in ultraviolet-B-inhibited pollen germination and tube growth of *Paulownia tomentosa* in vitro. *Physiologia Plantarum* 131: 273–282.
- Hepler PK, Vidali L, Cheung AY. 2001. Polarized cell growth in higher plants. *Annual Review of Cell and Developmental Biology* 17: 159–187.
- Holdaway-Clarke TL, Feijó JA, Hackett GR, Kunkel JG, Hepler PK. 1997. Pollen tube growth and the intracellular cytosolic calcium gradient oscillate in phase while extracellular calcium influx is delayed. *Plant Cell* 9: 1999–2010.
- Holdaway-Clarke TL, Hepler PK. 2003. Control of pollen tube growth: role of ion gradients and fluxes. *New Phytologist* 159: 539–563.
- Lancelle SA, Cresti M, Hepler PK. 1997. Growth inhibition and recovery in freeze-substituted *Lilium longiflorum* pollen tubes: structural effects of caffeine. *Protoplasma* 196: 21–33.
- Lanteri ML, Laxalt AM, Lamattina L. 2008. Nitric oxide triggers phosphatidic acid accumulation via phospholipase D during auxin-induced adventitious root formation in cucumber. *Plant Physiology* 147: 188–198.
- Lanteri ML, Pagnussat GC, Lamattina L. 2006. Calcium and calcium-dependent protein kinases are involved in nitric oxide- and auxin-induced adventitious root formation in cucumber. *Journal of Experimental Botany* 57: 1341–1351.
- Lazzaro MD, Cárdenas L, Bhatt AP, Justus CD, Phillips MS, Holdaway-Clarke TL, Hepler PK. 2005. Calcium gradients in conifer pollen tubes; dynamic properties differ from those seen in angiosperms. *Journal of Experimental Botany* 56: 2619–2628.
- Lazzaro MD, Donohue JM, Soodavar FM. 2003. Disruption of cellulose synthesis by isoxaben causes tip swelling and disorganizes cortical microtubules in elongating conifer pollen tubes. *Protoplasma* 220: 201–207.
- Lombardo MC, Graziano M, Polacco JC, Lamattina L. 2006. Nitric oxide functions as a positive regulator of root hair development. *Plant Signaling & Behavior* 1: 28–33.
- Lowenstein CJ. 2007. Nitric oxide regulation of protein trafficking in the cardiovascular system. *Cardiovascular Research* 75: 240–246.
- McInnis SM, Desikan R, Hancock JT, Hiscock SJ. 2006. Production of reactive oxygen species and reactive nitrogen species by angiosperm stigmas and pollen: potential signalling crosstalk? *New Phytologist* 172: 221–228.
- Morikawa H, Hayashi R, Senda M. 1978. Infrared analysis of pea stem cell walls and oriented structure of matrix polysaccharides in them. *Plant and Cell Physiology* 19: 1151–1159.
- Neill S, Barros R, Bright J, Desikan R, Hancock J, Harrison J, Morris P, Ribeiro D, Wilson I. 2008. Nitric oxide, stomatal closure, and abiotic stress. *Journal of Experimental Botany* 59: 165–176.
- Parre E, Geitmann A. 2005. Pectin and the role of the physical properties of the cell wall in pollen tube growth of *Solanum chacoense*. *Planta* 220: 582–592.
- Planchet E, Kaiser WM. 2006. Nitric oxide production in plants: facts and fictions. *Plant Signaling & Behavior* 1: 46–51.
- Prado AM, Colaço R, Moreno N, Silva AC, Feijó JA. 2008. Targeting of pollen tubes to ovules is dependent on nitric oxide (NO) signaling. *Molecular Plant* 1: 703–714.

- Prado AM, Porterfield DM, Feijó JA. 2004. Nitric oxide is involved in growth regulation and re-orientation of pollen tubes. *Development* 131: 2707–2714.
- Rockel N, Wolf S, Kost B, Rausch T, Greiner S. 2008. Elaborate spatial patterning of cell-wall PME and PME1 at the pollen tube tip involves PME1 endocytosis, and reflects the distribution of esterified and de-esterified pectins. *Plant Journal* 53: 133–143.
- Salmi ML, Morris KE, Roux SJ, Porterfield DM. 2007. Nitric oxide and cGMP signaling in calcium-dependent development of cell polarity in *Ceratopteris richardii*. *Plant Physiology* 144: 94–104.
- Šamaj J, Baluška F, Menzel D. 2004. New signalling molecules regulating root hair tip growth. *Trends in Plant Science* 9: 217–220.
- Schröder H. 2006. No nitric oxide for HO-1 from sodium nitroprusside. *Molecular Pharmacology* 69: 1507–1509.
- Silverman-Gavrila LB, Lew RR. 2003. Calcium gradient dependence of *Neurospora crassa* hyphal growth. *Microbiology* 149: 2475–2485.
- Yokota E, Muto S, Shimmen T. 2000. Calcium-calmodulin suppresses the filamentous actin-binding activity of a 135-Kilodalton actin-bundling protein isolated from lily pollen tubes. *Plant Physiology* 123: 645–654.

## Supporting Information

Additional supporting information may be found in the online version of this article.

**Fig. S1** Steepness was employed to describe the tip-focused  $\text{Ca}^{2+}$  gradient.

**Fig. S2** Effects of S-nitroso-N-acetylpenicillamine (SNAP), 2-(4-carboxyphenyl)-4, 4, 5, 5-tetramethylimidazoline-1-oxyl-3-oxide (cPTIO) and  $N_{\omega}$ -nitro-L-arginine (L-NNA) on the morphology of *Pinus bungeana* pollen tubes after treatment for 24 h.

**Video S1** The relative position of the electrode and pollen tube tip in the net  $\text{Ca}^{2+}$  flux experiment using the scanning ion-selective electrode technique (SIET).

**Video S2** Hepes buffer (the buffer for Calcium Green-1 indicator) was microinjected into normally growing pollen tubes as a control injection to determine whether injection affected pollen tube growth.

Please note: Wiley-Blackwell are not responsible for the content or functionality of any supporting information supplied by the authors. Any queries (other than missing material) should be directed to the *New Phytologist* Central Office.



## About *New Phytologist*

- *New Phytologist* is owned by a non-profit-making **charitable trust** dedicated to the promotion of plant science, facilitating projects from symposia to open access for our Tansley reviews. Complete information is available at [www.newphytologist.org](http://www.newphytologist.org).
- Regular papers, Letters, Research reviews, Rapid reports and both Modelling/Theory and Methods papers are encouraged. We are committed to rapid processing, from online submission through to publication 'as-ready' via *Early View* – our average submission to decision time is just 29 days. Online-only colour is **free**, and essential print colour costs will be met if necessary. We also provide 25 offprints as well as a PDF for each article.
- For online summaries and ToC alerts, go to the website and click on 'Journal online'. You can take out a **personal subscription** to the journal for a fraction of the institutional price. Rates start at £139 in Europe/\$259 in the USA & Canada for the online edition (click on 'Subscribe' at the website).
- If you have any questions, do get in touch with Central Office ([newphytol@lancaster.ac.uk](mailto:newphytol@lancaster.ac.uk); tel +44 1524 594691) or, for a local contact in North America, the US Office ([newphytol@ornl.gov](mailto:newphytol@ornl.gov); tel +1 865 576 5261).